TISSUE ENGINEERING: Part A
Volume 16, Number 5, 2010

DOI: 10.1089/ten.tea.2009.0616

Human Adipose-Derived Stromal Cells Accelerate Diabetic Wound Healing: Impact of Cell Formulation and Delivery

Peter J. Amos, B.S.,[1,*] Sahil K. Kapur, B.S.,[2,*] Peter C. Stapor, B.S.,[1,3] Hulan Shang, Ph.D.,[2] Stefan Bekiranov, Ph.D.,[4] Moshe Khurgel, Ph.D.,[5] George T. Rodeheaver, M.D.,[2] Shayn M. Peirce, Ph.D.,[1] and Adam J. Katz, M.D.[2]

Human adipose-derived stromal cells (ASCs) have been shown to possess therapeutic potential in a variety of settings, including cutaneous wound healing; however, it is unknown whether the regenerative properties of this cell type can be applied to diabetic ulcers. ASCs collected from elective surgical procedures were used to treat full-thickness dermal wounds in leptin receptor-deficient (*db/db*) mice. Cells were delivered either as multicellular aggregates or as cell suspensions to determine the impact of cell formulation and delivery methods on biological activity and *in vivo* therapeutic effect. After treatment with ASCs that were formulated as multicellular aggregates, diabetic wounds experienced a significant increase in the rate of wound closure compared to wounds treated with an equal number of ASCs delivered in suspension. Analysis of culture supernatant and gene arrays indicated that ASCs formulated as three-dimensional aggregates produce significantly more extracellular matrix proteins (e.g., tenascin C, collagen VI α3, and fibronectin) and secreted soluble factors (e.g., hepatocyte growth factor, matrix metalloproteinase-2, and matrix metalloproteinase-14) compared to monolayer culture. From these results, it is clear that cell culture, formulation, and delivery method have a large impact on the *in vitro* and *in vivo* biology of ASCs.

Introduction

Chronic wounds such as diabetic ulcers remain a significant global health burden despite concerted efforts toward their prevention and treatment. The prevalence of diabetes continues to increase as the population ages and obesity trends worsen. Nearly 11.8% of diabetic patients develop foot ulcers in their lifetimes, with an annual incidence approaching 2.5% of all diabetic patients.[1,2] Foot ulcers precede 84% of lower limb amputations in diabetic patients, making it the most common cause of amputation in those patients.[3]

Although the etiology and pathogenesis of diabetic wounds are variably understood, therapeutic strategies such as debridement, pressure relief, vascular optimization, and edema control are considered fundamental. Still, many wounds fail to heal despite adequate implementation of these wound care techniques. It is now well established that most, if not all, chronic wounds are characterized by a phenotypically altered cellular wound milieu. For example, both fibroblasts and endothelial progenitor cells from diabetic ulcers have been shown to exhibit impaired migration, proliferation, adhesion, and growth factor production.[4–6] This has led some to propose the application of fresh, unimpaired cells to nonhealing wounds as a means to reinitiate or replace the host tissue's wound-healing cascade.[7]

Emerging work suggests that adipose-derived stromal cells (ASCs) may be useful for therapeutic wound-healing applications.[8,9] In addition to their established multipotency,[10,11] ASCs secrete numerous growth factors that are known to favorably impact wound healing in both *in vitro* and *in vivo* wound-healing models.[12–16] Several groups have shown that human ASCs seeded onto acellular dermal scaffolds can facilitate healing in wounds of nude mice.[17–19] Similarly, other authors report that human ASCs are able to stimulate the proliferation and migration of dermal fibroblasts, enhance their production of matrix factors, and accelerate the re-epithelialization of wounds in nude mice.[20] Practically speaking, ASCs possess excellent translational qualities due to advantages of abundance, expendability, ease of harvest, and donor appeal. These considerations have led us to hypothesize that human ASCs possess the ability to improve the rate of healing in diabetic wounds, which are known to have cellular, growth factor, and matrix-related dysfunctions.

Mammalian cells normally exist within the context of a three-dimensional (3D) micro-milieu; yet, the majority of published literature describes the use of two-dimensional

Departments of [1]Biomedical Engineering and [2]Plastic and Reconstructive Surgery, University of Virginia, Charlottesville, Virginia.
[3]Department of Biomedical Engineering, Tulane University, New Orleans, Louisiana.
[4]Department of Biochemistry and Molecular Genetics, University of Virginia, Charlottesville, Virginia.
[5]Department of Biology, Bridgewater College, Bridgewater, Virginia.
*These two authors contributed equally to this work.

(2D) adherent monolayer culture for mesenchymal cells. Extracellular matrix (ECM) is known to play a critical role in tissue repair, serving as a scaffold and as a modulator of cell function and growth factor functionality.[21,22] Cells cultured in adherent monolayers ultimately need to be lifted into suspension for further handling/manipulation, but this process disrupts any ECM milieu that may have been established. Therefore, we also hypothesize that ASCs prepared and delivered as 3D multicellular aggregates (MAs) will exhibit enhanced biological and therapeutic properties compared to cells prepared using traditional monolayer techniques and delivered as cell suspensions.

In summary, diabetic ulcers are a common and devastating complication for the world's growing population of diabetic patients. Although the use of ASCs for the treatment of diabetic ulcers is an attractive strategy, it requires further evaluation. The objectives of this study were to examine whether human ASCs have the ability to improve the rate of wound healing in genetically diabetic mice and whether ASC formulation and delivery methods impact biological activity and therapeutic effect.

Methods

Cell isolation and preparation

All adipose tissue was obtained from either intraoperative suction lipectomy or laboratory liposuction of panniculectomy specimens. Subcutaneous adipose tissue was obtained from nondiabetic patients undergoing elective surgical procedures in the Department of Plastic Surgery at the University of Virginia via a protocol approved by The University of Virginia's Human Investigation Committee. ASCs were isolated using previously described methods.[23] Briefly, harvested tissue was washed with complete Hanks buffer, centrifuged, decanted to remove oil, and then enzymatically dissociated. The dissociated tissue was filtered to remove debris, and the resulting cell suspension was centrifuged. Pelleted stromal cells were then recovered, washed twice, filtered twice (250 μm mesh followed by 105 μm mesh), centrifuged, and decanted. Contaminating erythrocytes were lysed with an osmotic buffer, and the stromal cells were plated onto culture plastic (Thermo Fisher Scientific, Rochester, NY). Cultures were washed with buffer 24–48 h after plating to remove unattached cells and then re-fed with a fresh medium. The initial plating medium consisted of Dulbecco's modified Eagle's medium/F12 with 10% fetal bovine serum and 1% antibiotic–antimycotic. Cultures were maintained at 37°C with 5% CO_2 and fed two to three times per week. Cells were grown to confluence after the initial plating ($p = 0$), typically within 10–14 days. At confluence, $p = 0$ cells were lifted using TrypLE (Invitrogen, Carlsbad, CA) and counted on a hemacytometer using trypan blue exclusion.

MA preparation

Passage zero ($p = 0$) cells were labeled with anti-CD31 and anti-CD45 antibodies (BD Biosciences, San Jose, CA), and magnetic sorting (MACS Miltenyi Biotec, Auburn, CA) was used to remove mature endothelial cells and leukocytes. The resulting CD31−/CD45− cells were collected and replated as passage 1 ($p = 1$) cells. After 2 weeks of culture, the cells were released, counted, and resuspended at a concentration of 625,000 cells/mL in a growth-factor-enriched low-serum medium (Dulbecco's modified Eagle's medium/F12, 0.1 mM L-glut, 10^{-8} M dexamethasone, 100 μM ascorbic acid 2-phosphate, 0.50% ITS+3, 0.05% fatty acid supplement, 1% nonessential amino acids, 10^{-8} M estradiol, 10^{-8} M progesterone, 500 ng/mL hydrocortisone, 10 ng/mL epidermal growth factor, 1 ng/mL platelet-derived growth factor, 1 ng/mL stem cell growth factor-beta (SCGF-β), 1 ng/mL tumor necrosis factor-alpha (TNF-α), 1 ng/mL interleukin 1β [IL-1β], and 1% antibiotic–antimycotic) with 1% human serum (AR10-1%HS).[24] Forty-microliter droplets were placed on the inside of a culture dish lid, and the lid was inverted to induce MA formation using the hanging droplet method.[25,26] Cells in the resulting hanging droplets were allowed to form 3D aggregates comprised of 25,000 cells per droplet. After 24 h of culture, MAs were transferred into suspension culture in ultra low attachment (ULA) culture plates (Corning, Lowell, MA). Separate aliquots of the same CD31-/CD45- ASCs were cultured as adherent monolayers, using standard culture dishes, and the same low-serum (AR10-1%HS) medium was used to culture MAs. Both MAs and monolayer cells were cultured for 1 week in the low-serum medium before use in *in vitro* and *in vivo* studies.

ASC mRNA expression

To evaluate the gene expression profile of ASCs grown as MAs in suspension culture relative to ASCs grown as adherent monolayers, human ASCs from three different women, with an average age of 37 and an average body mass index (BMI) of 30 (donor 1: 34 years old, BMI 25.1; donor 2: 45 years old, BMI 28.2; donor 3: 31 years old, BMI 35.4), were used. After isolation, ASCs were initially expanded as monolayers in the AR10-1%HS medium and split into two equal groups. One group of cells was lifted and placed back into monolayer culture at 2000 cells/cm^2, whereas the other group was formed into MAs (25,000 ASCs/MA) and transferred to suspension culture. The fresh medium was provided for all cultures on day 3. On day 6, cells were harvested from both groups and RNA was isolated using a commercially available kit (PureLink Micro-ti-Midi Total RNA Purification System, Cat no. 12183-018). From each of the three different donors, ASCs grown as monolayers and ASCs grown as MAs were analyzed in triplicate using separate Affymetrix human gene chips (HgU133 plus 2.0; $n = 9$/experimental group). An Agilent BioAnalyzer was used to ensure the quality of each total RNA sample. Background intensity was derived from the intensity values of the lowest 2% of cells on the chip, establishing an overall baseline intensity that was subtracted from all cells before gene expression levels were calculated. Noise levels were derived from the standard deviation of the background intensity measurements. A parallel culture of each experimental group (monolayer and MA) was used to quantify the number of cells in each sample. Arrays were analyzed as described below. To develop a more macroscale understanding of data variability, a principal component analysis of all gene array data was performed.

Proteomic analysis

The translational profile of ASC MAs was evaluated using ELISA to quantify soluble factors secreted by the cells, and mass spectrometry to evaluate proteins within the aggre-

gates. ASCs were prepared in parallel groups of adherent monolayers and suspension-cultured MAs as described above. The MAs were placed into suspension culture in 6-well ULA plates (day 0) and maintained in AR10-1%HS. In parallel, monolayer-cultured ASCs were re-plated at 2000 cells/cm^2 in adherent monolayer culture (day 0). The conditioned medium was then collected (and the fresh medium replaced) from each group on postplating days 3. The day 3 supernatant from each of six wells was combined and frozen for subsequent quantitative ELISA analysis of growth factor levels. Each sample was analyzed in duplicate by Pierce Biotechnology's Searchlight™ service (using CLIA-certified practices and protocols). Fresh samples of each culture medium were analyzed in parallel for baseline levels of growth factors, and these values were subtracted from the culture-conditioned samples. Parallel cell cultures were counted to determine the number of cells per monolayer sample or cells per aggregate and then used to normalize ELISA results.

Analysis using liquid chromatography mass spectrometry was done with a Finnigan LTQ-FT system and a Protana nanospray ion source. Ten microliters of prepared protein-gel extract was injected, and peptides were eluted from the column by an acetonitrile/acetic acid gradient at a flow rate of 0.25 μL/min over 2 h. The proteins expressed by the monolayers and MAs were compared on days 3 and 6, and care was taken so that no exogenous proteins were added to the samples.

Full-thickness diabetic wound model

Male diabetic BKS.Cg-$m^{+/+}$ $Lepr^{db}$/J (*db*/*db*) mice (Jackson Laboratories, Bar Harbor, ME) were acclimated before experimentation. Hyperglycemia was verified for each animal before wounding using an Accu-Chek Compact digital glucose meter (Roche Diagnostics, Indianapolis, IN) to confirm that each animal had a circulating blood glucose concentration of at least 250 mg/dL.

On the day of wounding, the dorsa of animal subjects were depilated and a circular full-thickness excisional wound of 1 cm diameter (approx. 78.5 mm^2 area) was made using a template.[27] Nondiabetic heterozygote littermates (*db*/+) received an identical injury. A small ruler was placed in the plane of the wound, and images were taken of the wounds using a 5.0 megapixel digital camera. After image acquisition, either cellular (ASC suspension in diabetic mice, ASC MA in diabetic mice) or vehicle (phosphate-buffered saline [PBS] in diabetic mice, PBS in nondiabetic mice) treatment was administered to the wounds. ASCs for *in vivo* studies were derived from a single 49-year-old woman with a BMI of 27.4. Blinding was intended, but proved impossible due to the macroscopic visibility of MAs and obvious size differences between homozygous and heterozygous mice. In each cellular group, approximately 350,000 cells were delivered to each wound. For wounds receiving ASCs in MA form, 14 MAs formed from 25,000 cells each were administered per wound. Cellular treatments were delivered using 100 μL of PBS, and a matching volume of PBS was delivered as a vehicle control treatment. All cells were used at $p = 1$. After treatment, benzoin was painted around the wound on the surrounding uninjured tissue before application of Tegaderm™ bandages (3M, St. Paul, Minnesota), being careful not to allow any benzoin to come near the wounds' edges. Tegaderm bandages were applied to each wound without allowing any delivered material (PBS or cells) to leak out of the wound area. Coban™ wrap (3M) was cut to fit around the waist of the animals to prevent the mice from scratching the Tegaderm bandages off, but loose enough to allow the animals to breathe and move comfortably.

On postwounding days 5, 7, 9, 12, 14, 16, 19, and 21, the Tegaderm and Coban bandages were carefully removed, being sure that the size of the wound and any epithelialization present were not disturbed. Wounds were imaged at each of these time points in a similar manner to the day of wounding and quantified using Image J software (NIH). Each postwounding measurement was normalized to its corresponding day 0 wound area and recorded as a percentage of the original wound remaining open. Validation of area measurements was performed by using a stencil to draw a perfect circle with a diameter of 13/32 inches (an area equal to 83.62653 mm^2 as measured with the perfect circle tool in Image J). After 10 freehand measurements performed in an identical way as measurements of wound sizes in this study's experiments, an average measured area of 83.3713 mm^2 and a standard deviation of 1.287137 mm^2 was obtained.

Using an identical technique, five MAs formed from 25,000 cells each were also delivered to a separate group of *db*/*db* mice to comprise a low-dose experimental group (125,000 cells per wound). Animals receiving low-dose MA treatments were imaged and analyzed using the same protocol as all other ASC experiments.

Statistical analysis

Gene arrays were quantile normalized, and gene chip robust multiarray averaging was applied to estimate $\log_2$ gene expression levels.[28] A list of genes expressed differentially between monolayer and MA was obtained using the Limma Bioconductor package, which implements a modified *t*-test.[29] Multiple hypothesis testing was accounted for by applying a false discovery rate correction to the *p*-values and using a 5% false discovery rate cutoff.

All results from *in vivo* studies are presented in the form of mean ± standard deviation. These comparisons were made using the statistical analysis tools provided by SigmaPlot 5.0 (Systat, Point Richmond, CA). Using a Power Analysis, we calculated that the number of animals per study group ($n = 8$) yields a power of 0.80 with $\alpha = 0.05$ based on an estimated difference in mean wound area of 14 mm^2 and an expected standard deviation of 8 mm^2. Wound-healing rate data were analyzed for statistical significance using only data collected between days 0 and 12 (the open wound interval) since all wounds, regardless of experimental group, were fully healed after 12 days and because the *db*/*db* model is best suited to evaluate treatments that affect the early phases of wound healing.[30] Animals that partially removed the Tegaderm bandage or developed an infection at any point during the experiment were removed from consideration in data analysis (MA group: 3; vehicle diabetic group: 3; monolayer ASC group: 3; nondiabetic group: 4). Two-way ANOVA analysis followed by Tukey's multiple comparisons test was used to determine significance between healing rates for each study group, allowing for comparison of healing rates over the course of 12 days rather than a comparison of wound size at each individual time point. Therefore, average wound size as a function of both treatment group and time was compared for the four groups, resulting in an analysis of each treatment's

effect on wound size over the entire 12-day open wound interval. Statistical significance was asserted at $p < 0.05$.

Results

MA delivery system characterization

It was observed that the size and number of MAs formed per hanging droplet were dependent on the concentration of ASCs used. At concentrations of approximately 5000 cells/droplet (or 125,000 cells/mL) or higher, MAs formed with very little variability in aggregate size (Fig. 1), but when lower concentrations were used, MA formation was much less uniform. It was also noted that after several days in culture, the MAs were difficult to dissociate using purely mechanical means; in fact, enzymatic strategies became necessary for dissociation. Upon plating on standard tissue culture plastic, the MAs readily adhered and gave rise to confluent monolayers of cells with plasticity toward adipose, cartilage, and bone phenotypes (data not shown). A single aggregate could subsequently be serially lifted and re-plated at least 20 times, giving rise to adherent monolayer cells with proliferative capacity on each re-plating.

mRNA expression of ASCs in monolayer culture versus MA culture

Isolated RNA was found to be of high quality for all specimens. A quantification of cell numbers from parallel cultures of MAs and monolayers showed no statistical difference in the number of ASCs in each group at the time of RNA isolation (1.56×10^6 cells/sample for MA cultures, 1.40×10^6 cells/sample for monolayer cultures). When mRNA expression of ASCs in MAs was compared to ASCs in monolayer culture, ASCs in MAs were found to express thousands of genes at a significantly higher level than ASCs in monolayers. Over 35 wound-healing-related genes were upregulated in ASCs cultured as MAs compared to those cultured in monolayers (Table 1, $p < 0.05$).

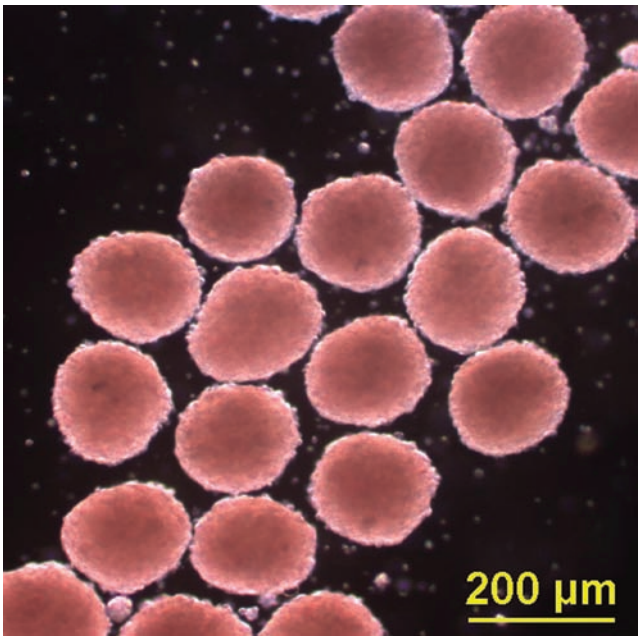

FIG. 1. Multicellular aggregates (MAs) formed from human adipose-derived stromal cells (ASCs). Aggregates formed in hanging droplets from solutions of at least 125,000 cells/mL showed very little variability in final diameter, but lower concentrations produced aggregates with much more variability in diameter. MAs also showed more resistance to mechanical dissociation than monolayer-cultured ASCs. Color images available online at www.liebertonline.com/ten.

Principal component analysis revealed a separation along the first principle component (PC1 along the x-axis) or major axis of variation between MA and monolayer-cultured samples independent of donor (Supplemental Fig. S1, available online at www.liebertonline.com/ten). The individual patient gene expression profiles were separated along the second principle component (PC2 along the y-axis) or the secondary axis of variation independent of culture condition. In Supplemental Figure S2 (available online at www.liebertonline.com), the distribution of the $\log_2$ ratio of the MA ASC gene expression standard deviation over monolayer-cultured ASC gene expression standard deviation illustrates a relatively large population of genes for which the standard deviation is approximately twofold smaller in ASCs formed into MAs as compared to ASCs grown as monolayers.

Protein production of ASCs in monolayer culture versus MA culture

Secreted protein production (fraction unbound to ECM) was increased in ASC MAs as compared to ASC monolayers. ELISAs showed that supernatant concentrations of fibrinogen, tissue inhibitor of metalloproteinase-1, matrix metalloproteinase-2 (MMP2), transforming growth factor-β1, basic fibroblast growth factor, insulin-like growth factor binding protein-1, keratinocyte growth factor (KGF), epidermal growth factor, hepatocyte growth factor, and vascular endothelial growth factor were higher in MAs compared to monolayers (Fig. 2). Fibronectin secretion showed the highest secretion levels (by mass) in monolayer and MA culture (9.87 pg/cell/3 days and 18.88 pg/cell/3 days, respectively). The inflammatory proteins IL-6, IL-8, and monocyte chemoattractant protein 1, however, were secreted in lower amounts when ASCs were cultured as MAs instead of as monolayers. Mass spectrometry studies demonstrated increased production of matrix-related proteins (MMP14, MMP2, Tenascin C, Collagen VI α3, and Fibronectin 1) in MAs (Fig. 3).

Impact of delivery method on diabetic wound healing

Animals in all groups healed over 90% of their original dermal wound areas by day 12 of the experiment (Fig. 4, see also, Supplemental Fig. S3, available online at www.liebertonline.com/ten). Two-way ANOVA statistical analysis showed that diabetic mice receiving a vehicle delivery of sterile PBS ($n = 8$) healed at a slower rate during the first 12 days of the experiment than nondiabetic mice ($n = 4$) treated with the same volume of sterile PBS ($p < 0.001$). Diabetic animals receiving a dose of ASCs in suspension ($n = 8$) also healed at a slower rate than nondiabetic vehicle-treated control animals ($p < 0.001$). Moreover, there was no statistical difference between the healing rates of diabetic mice dosed with ASCs in single-cell suspensions and age-matched diabetic mice receiving vehicle treatment. In contrast, the

Table 1. Gene Expression Levels When Adipose-Derived Stem Cells Are Cultured as Multicellular Aggregates Relative to Monolayer Culture

Mean expression level in 2D culture (relative fluorescence intensity)	*Fold change from 2D culture to 3D culture*	*Description*	*Putative role in wound healing*	
10.23	−3.56	Angiopoietin-1	Modulator of angiogenesis	Angiogenesis ↑ Inflammation ↓
7.05	23.43	Angiopoietin-like 2	Modulator of angiogenesis	
4.89	17.15	Bradykinin receptor B1	Modulator of inflammation	
5.93	11.31	Hepatocyte growth factor	Modulator of angiogenesis, endothelial cell mitogen	
5.02	13.83	Endothelin receptor type A	Modulator of vascular tone	
8.51	5.10	Stromal-cell-derived factor-1 (SDF-1)	Cytokine involved in recruitment of inflammatory cells and circulating progenitor cells	
10.62	2.58	Platelet-derived growth factor receptor β	Modulator of angiogenesis, vascular stabilization, and fibroblast proliferation	
12.48	−7.89	Thrombospondin-1	Mediates cell-to-cell and cell-to-matrix interactions, modulator of angiogenesis, and platelet aggregation	
2.41	57.28	Insulin-like growth factor 1 (IGF-1)	Regulator of cell proliferation	↑
5.02	31.34	Insulin-like growth factor binding protein 5	Regulator of cell proliferation	
9.94	28.84	Periostin	Regulator of cell proliferation	
5.47	6.15	RAS homolog gene family, member J (RHO J)	Regulator of cell migration	
8.92	1.28	TGF-β1	Regulator of cell proliferation and differentiation	Morphogenesis
4.69	5.35	TGF-β3	Regulator of cell proliferation and differentiation	
3.22	2.28	Syndecan 1	Transmembrane heparan sulfate proteoglycan that mediates cell binding and cell signaling and is important in modulating proliferation, migration, and cell–matrix interactions	
9.37	2.07	Syndecan 2	Transmembrane heparan sulfate proteoglycan that mediates cell binding and cell signaling and is important in modulating proliferation, migration, and cell–matrix interactions	↓
7.60	21.11	Biglycan	Proteoglycan that interacts with collagen (e.g., Type II), binds TGF-β, and is abundant in connective tissue	↑
2.35	10.48	Collagen, type VIII, α2	Protein that is abundant in connective tissue and an important component of basement membrane	
2.65	86.82	Collagen, type XIV, α1	Protein that is abundant in connective tissue and an important component of basement membrane	
6.03	29.24	Collagen, type XV, α1	Protein that is abundant in connective tissue and an important component of basement membrane	
6.48	6.11	Collagen, type XVIII, α1	Protein that is abundant in connective tissue, and the proteolytically produced C-terminal fragment, endostatin, is an antiangiogenic agent	

(*continued*)

Table 1. (Continued)

Mean expression level in 2D culture (relative fluorescence intensity)	*Fold change from 2D culture to 3D culture*	*Description*	*Putative role in wound healing*	
13.73	1.95	Collagen, type VI, α3	Protein that is a major structural component of microfibrils in the ECM	
11.13	1.24	Decorin	An important component of connective tissue that binds to type I collagen fibrils, and plays a role in matrix assembly	
5.58	1.56	Elastin	Component of connective tissue that assists with load-bearing and storing mechanical energy	ECM deposition and remodeling
15.03	1.08	Fibronectin 1	Protein abundant in ECM and important in mediating cell signaling	
6.90	10.06	Fibronectin type III domain containing 1	Protein abundant in ECM and important in mediating cell signaling	
9.65	1.53	Fibronectin type III domain containing 3A	Protein abundant in ECM and important in mediating cell signaling	
5.49	5.86	Laminin, α1	Glycoprotein important in basement membrane	
11.90	1.77	Laminin, β1	Glycoprotein important in basement membrane	
9.74	13.93	MMP1	Collagenase	
12.95	2.19	MMP2	Gelatinase	
3.84	13.55	MMP8	Collagenase	
3.28	30.70	MMP9	Gelatinase	
8.66	1.68	MMP14	Membrane-type MMP; activates MMP2	
13.37	2.16	TIMP 1	Glycoprotein that inhibits MMPs	
12.97	1.87	TIMP 2	Glycoprotein that inhibits MMP 2 and MMP14	
8.58	4.00	TIMP 3	Glycoprotein that inhibits MMPs	
8.79	13.00	Tenascin C	Glycoprotein that is abundant in ECM and implicated in wound healing	

ECM, extracellular matrix; TGF-β1, transforming growth factor β1; MMP1, matrix metalloproteinase 1;TIMP 1, tissue inhibitor of matrix metalloproteinase 1.

wounds of diabetic mice treated with ASCs in MAs ($n = 8$) decreased in size faster than both vehicle-treated diabetic mice and diabetic mice receiving ASCs in suspension ($p < 0.001$). The healing rates between nondiabetic control mice and diabetic mice treated with ASCs in MAs were statistically similar during the 12-day time frame. When a lower dose of 125,000 ASCs was delivered as MAs to diabetic wounds of the same size ($n = 7$), the decrease in open wound size over the first 12 days was statistically similar to that of vehicle-treated diabetic wounds (data not shown).

Discussion

Our results show that the administration of human ASCs can accelerate the closure of dermal wounds on diabetic mice to a rate approaching that of vehicle-treated healthy, nondiabetic mice. Specifically, this therapeutic effect was seen only when ASCs were prepared and delivered as suspension-cultured 3D MAs, but not when delivered as cell suspensions derived from monolayer culture. These results demonstrate that cell preparation and delivery method have a nontrivial impact on the phenotype, biological activity, and *in vivo* therapeutic capacity of cell-based strategies.

Both the initial formulation and subsequent nonadherent culture of MAs are guided by the principal of self-assembly and self-maintenance. With this approach there are no subjective judgments about when cells are confluent, or subconfluent and in need of passage. It is therefore interesting, but not surprising, that our data demonstrate that ASCs cultured as MAs have a more consistent and reproducible transcriptome than monolayer ASCs. In essence, the MA culture system seems to diminish donor-to-donor variability that is characteristic of primary cells cultured as monolayers, and this may have important implications for translational efforts.

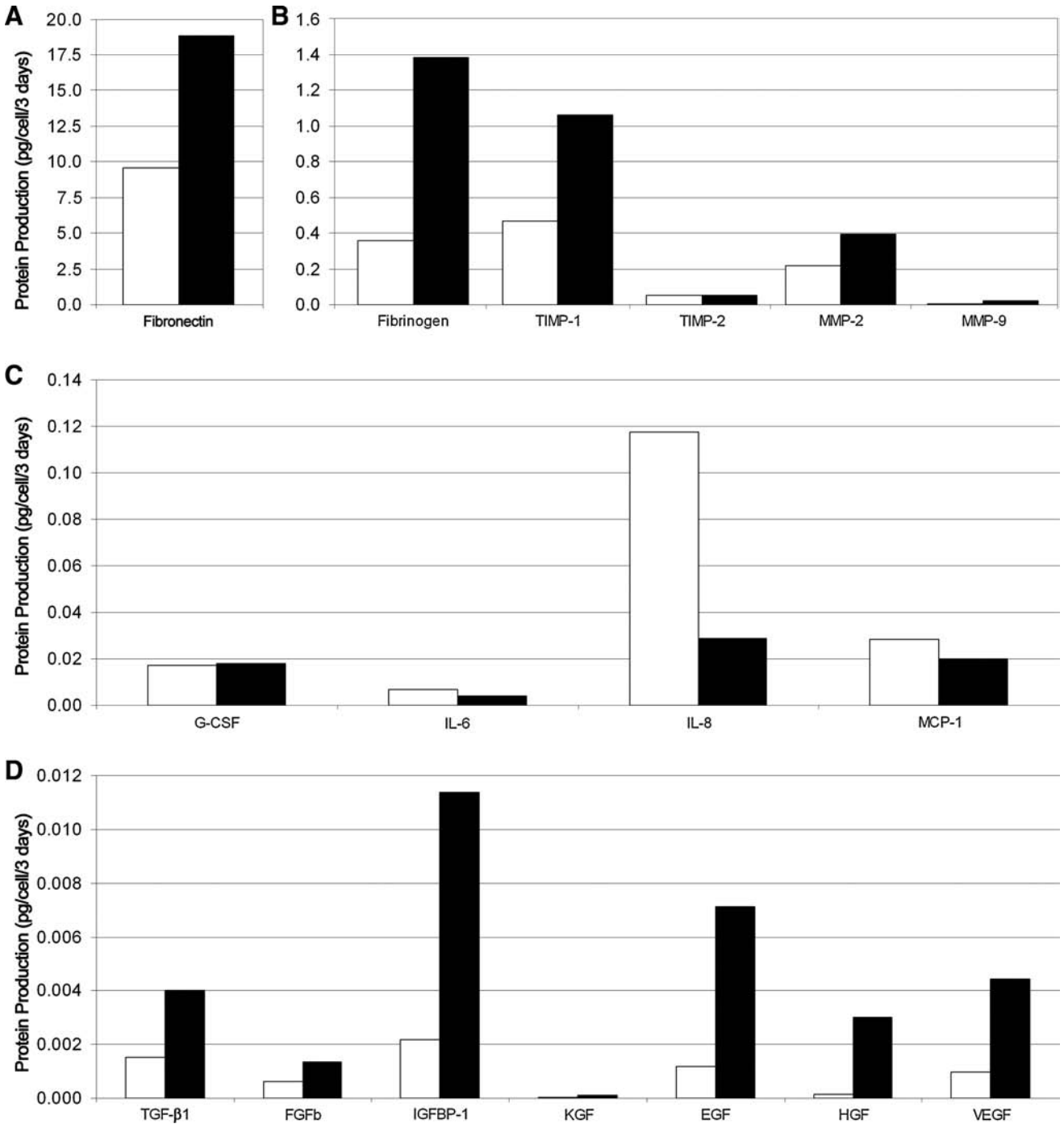

FIG. 2. ELISA analysis of wound-healing protein production by ASCs when cultured as MAs compared to monolayer culture. The secretion of several proteins linked to angiogenesis, regeneration, and extracellular matrix remodeling was found to be higher when ASCs were cultured as three-dimensional MAs (black bars) rather than in normal two-dimensional monolayers (white bars; **A, B, D**). In contrast, secretion of inflammatory proteins such as interleukin 6 (IL-6), interleukin 8, and monocyte chemoattractant protein-1 was increased in monolayer culture relative to MA culture (**C**).

It is important to recognize that there is no animal model that perfectly mimics the chronic, nonhealing nature of human diabetic wounds. Unlike humans, loose-skinned animals like mice heal 90% or more of their wounds by contraction, whereas epithelialization accounts for only about 10% of closure.[31,32] Still, the use of *db/db* mice as a model of delayed wound healing is well established in the literature.[33–36] The *db/db* wound model is particularly suited to interventions that stimulate the early phases of healing and replace or enhance the levels of various growth factors that are known to be diminished in diabetic healing.[30] Although animal models of healing have limited direct correlation to human chronic wounds, the ability to stimulate or enhance wound contraction of human diabetic wounds has significant clinical impact.

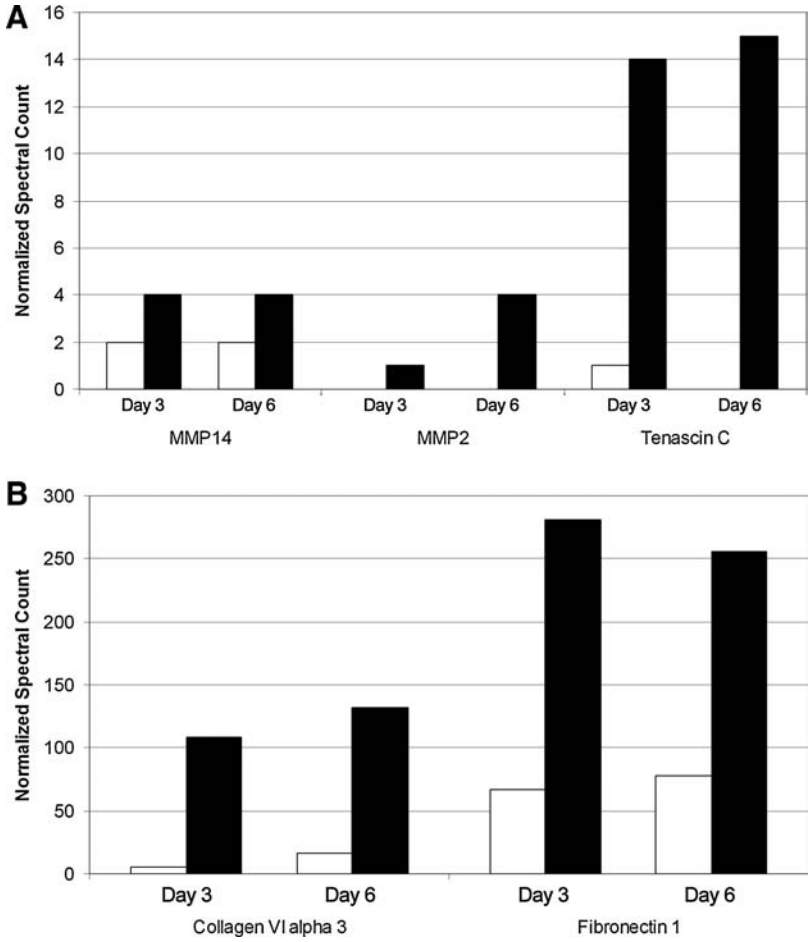

FIG. 3. Mass spectrometry analysis of matrix-related protein production by adipose-derived stromal cells (ASCs) when cultured as multicellular aggregates (MAs) compared to monolayer culture. Mass spectrometry data is consistent with gene array data in that increases are seen for each protein (**A:** MMP14, MMP2 and Tenascin C; **B:** Collagen and Fibronectin), analyzed when ASCs are cultured as MAs rather than as monolayers. There is no obvious trend for production of these proteins over time from data obtained after three and six days in culture.

Human diabetic wounds take a very long time to heal, if they do heal at all. If these aggregates were to cause closure of human wounds through contraction, or any other means, the clinical outcome would be more favorable than an unhealed wound. Certainly, the microscopic extent of epithelialization is difficult to discern by gross examination, and this may explain the relatively large standard deviations in our data (Fig. 4). With this understanding, our results provide compelling evidence that the formulation and delivery of ASCs as 3D aggregates significantly and favorably impacts their genotype, phenotype, biological potency, and *in vivo* therapeutic effect in the early phases of wound healing.

Of interest, related trials in which mice were treated with a lower cell dose of ASC MAs showed that wounds did not exhibit significant acceleration of healing over vehicle-treated controls (data not shown). This suggests that, in addition to cell formulation, cell dose also impacts therapeutic effect. The fact that no improvement in healing rate is observed after decreasing the number of MAs administered to the wound by approximately two-thirds of the original dose suggests a dose–response relationship involving ASC formulation and delivery and is consistent with published data.[37]

The 3D formation and culture of ASCs may also enhance their biological activity and efficacy via a number of mechanisms, including the increased release of paracrine signals or by ECM delivery, production, and remodeling. Each has the potential to facilitate cell survival, migration, proliferation, differentiation, and/or angiogenesis/arteriogenesis. Indeed, many of the genes and proteins found to be upregulated in our studies of ASC MAs (Table 1, Figs. 2 and 3) have been shown to be important for diabetic wound healing.[15,16,38–42] It is, therefore, reasonable to hypothesize that the observed increase in the production of these proteins plays at least a partial role in the increased rate of diabetic wound healing associated with ASC MA treatment. The synergistic interactions between growth factors and ECM proteins (in particular those involving growth factors and ECM components upregulated in MAs like insulin-like growth factor binding protein-1, transforming growth factor-β1, vascular endothelial growth factor, hepatocyte growth factor, decorin, biglycan, and fibronectin) are increasingly being recognized as playing a significant role in wound healing and tissue repair,[13,21,43–50] and although the secreted protein values reported in this paper do not reflect the full effect of the synergy and sequestration of secreted proteins (proteins sequestered by ECM are not interrogated by ELISA techniques), it is probable that such signaling plays a role in the enhanced *in vivo* activity of ASCs formulated as MAs relative to ASC suspensions.

The upper size limit observed for MAs is largely independent of the initial number of cells used in MA formation and is likely determined by protein and nutrient diffusion to core cells. Although hematoxylin and eosin and bromodeoxyuridine (data not shown) staining demonstrate viable cells in the

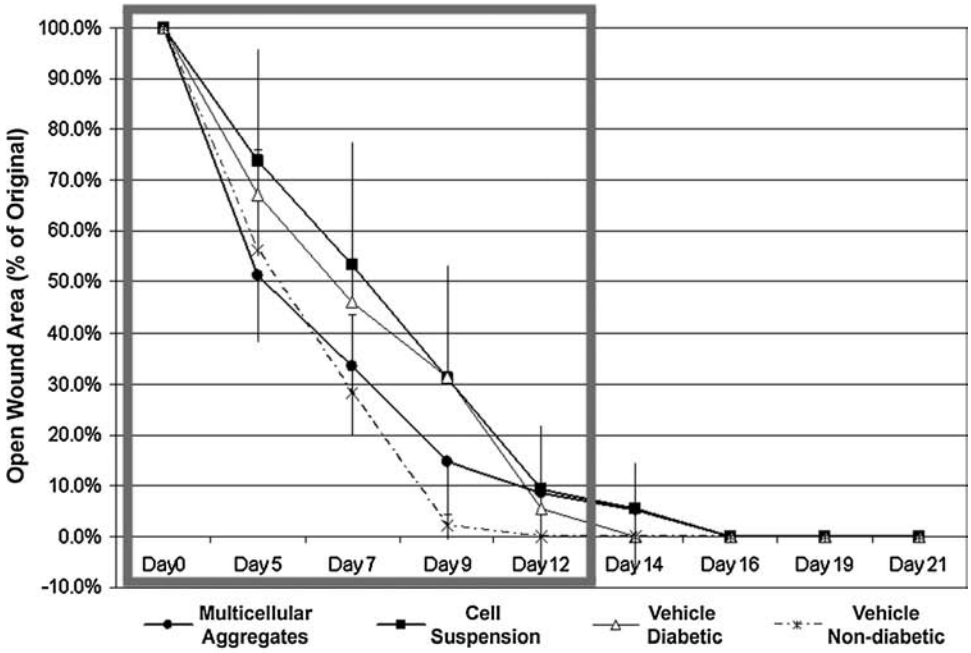

Time Point	Treatment Group	Average Open Wound Area (mm^2)	Average Open Wound Area (%)
Day 5	Nondiabetic Vehicle	33.4	56.3%
	ASC MA	35.0	51.2%
	ASC Suspension	51.5	73.8%
	Diabetic Vehicle	43.1	67.3%
Day 9	Nondiabetic Vehicle	1.3	2.2%
	ASC MA	10.5	14.6%
	ASC Suspension	21.8	31.1%
	Diabetic Vehicle	19.8	31.3%

FIG. 4. Comparison of diabetic wound closure over time after treatment with ASCs delivered in suspension or formulated as MAs. Wounds in all groups heal to 90% of original by day 12. During this 12-day open wound interval (gray rectangle), ASCs formed into MAs healed wounds at a significantly faster rate than either ASCs in suspension or vehicle-treated diabetic mice ($p < 0.001$). Diabetic wounds treated with ASC MAs also healed at a statistically similar rate to wounds inflicted on nondiabetic, vehicle-treated littermates over the same open wound interval. Both vehicle-treated diabetic wounds and cell-suspension-treated wounds healed at a statistically slower rate than nondiabetic controls within the open wound interval ($p < 0.001$).

core of MAs, it is likely that cells in this location are experiencing hypoxic conditions. This, in turn, could stimulate changes in gene transcription and protein translation that alter phenotype and biological activity.[51] Alternatively, it is possible that the delivery of ASCs to diabetic wounds as MAs may be useful for the simple reason that it keeps the ASCs from dispersing and spatially diluting the number of ASCs per area of wounded tissue.

It is likely that MA formulation increases the benefit of incorporated cells in the context of diabetic wound healing through a variety of mechanisms, including, but not limited to, cell–cell signaling, cell–matrix signaling, and possible hypoxic preconditioning of cells within the core of the MAs.[13,52] The concurrence of these cues is probably important for the overall increase in wound healing speed, but it is worth exploring which of these activation cues resulting from MA formulation is of primary importance.

Conclusions

In this study, we have shown that the self-directed formation and culture of ASCs as MAs significantly changes their

transcriptional profile and their biological potency (both *in vitro* and *in vivo*) as compared to cells grown in traditional monolayer. One possible mechanism by which this improvement is effected is an increase in ASC protein and ECM secretions caused by culturing the ASCs as 3D MAs. A potential alternative and complementary pathway for increased diabetic wound closure speed is long-term wound engraftment of delivered cells, with potential for subsequent *in vivo* differentiation to relevant cell lineages. Both of these mechanisms are supported by the genetic and protein analyses performed in this study, as genes and proteins related to migration, proliferation, angiogenesis, and ECM deposition were upregulated. Although ASCs have been observed investing directly in wounded skin in immunocompromised mice,[17] no histological evidence has been acquired to this point evaluating physical positioning and engraftment of ASCs in diabetic wounds over time, or that such incorporation is the primary mechanism of regeneration. Further, existing literature indicates that xenogeneic, allogeneic, and syngeneic cells do not survive for extended periods in immunocompetent hosts, despite successful healing of a wound.[37,53]

ASCs have been shown to have regenerative effects both through secretion and differentiation pathways in other systems,[54] so their action in diabetic wound healing may be through a similar mechanism. To further investigate the exact mechanisms by which ASCs accelerate diabetic wound healing, in-depth histological analysis of ASC engraftment, morphology, and lineage marker expression could be performed using autologous or syngeneic donor cells. Since bone-marrow-derived stem cells have also been shown to improve wound healing, a comparison of wound-healing kinetics and mechanisms in diabetic wounds treated with ASCs and wounds treated with bone-marrow-derived stem cells would be informative. In future studies, comparisons to both fibroblasts grown as aggregates and commercially available wound-healing products (such as Apligraf® and Dermagraft®)[55,56] could serve to provide important mechanistic insights into, as well as expose differentiating aspects between these varying approaches to cell-based wound therapy. Finally, it may be worthwhile to confirm our current findings in a larger animal model in which wounds of a more clinically relevant size could be evaluated.

Acknowledgments

The authors would like to thank Dr. Anna Parker for her extensive help in the development of protocols regarding *in vivo* wound-healing experiments, Dr. Roy and Rebecca Ogle and Robin Felder for use of equipment and assistance with imaging for these studies, the surgical residents and staff in the University of Virginia Department of Plastic Surgery for facilitating the accrual of tissue for research, and the University of Virginia Biomolecular Research Facility for technical assistance in carrying out gene chip analysis. This work was supported by the University of Virginia Department of Biomedical Engineering, the University of Virginia Department of Plastic Surgery, the Wallace H. Coulter Foundation (A.J.K. and S.M.P.), the National Institutes of Health Grant 1R21HL091312-01 (S.M.P. and A.J.K.) and Grant R21HL72141 (A.J.K.), the Armed Forces Institute of Regenerative Medicine (A.J.K.), and a personal gift from Dr. and Mrs. Peyton Weary.

Supplemental Methods

Gross histology of wounds

Wound sites were excised at day 21, fixed with 0.4% paraformaldehyde, embedded in paraffin, and sectioned perpendicularly to the skin surface. Hematoxylin and eosin staining was performed by the University of Virginia Histology Core Facility before mounting.

Disclosure Statement

P.J.A., S.K.K., H.S., P.C.S., S.B., G.T.R., and S.M.P.: no competing financial interests exist.

A.J.K.: named inventor on issued and pending patents related to the isolation and use of adipose-derived stem cells, matrix, and other adipose-related technologies and is engaged in efforts to commercialize such.

References

1. Abbott, C.A., Carrington, A.L., Ashe, H., Bath, S., Every, L.C., Griffiths, J., Hann, A.W., Hussein, A., Jackson, N., Johnson, K.E., Ryder, C.H., Torkington, R., Van Ross, E.R.E., Whalley, A.M., Widdows, P., Williamson, S., and Boulton, A.J.M. The North-west diabetes foot care study: incidence of, and risk factors for, new diabetic foot ulceration in a community-based patient cohort. Diabet Med **19,** 377, 2002.
2. Brem, H., Tomic-Canic, M., Entero, H., Hanflik, A.M., Wang, V.M., Fallon, J.T., and Ehrlich, H.P. The synergism of age and db/db genotype impairs wound healing. Exp Gerontol **42,** 523, 2007.
3. Pecoraro, R.E., Reiber, G.E., and Burgess, E.M. Pathways to diabetic limb amputation: basis for prevention. Diabetes Care **13,** 513, 1990.
4. Loot, M.A., Kenter, S.B., Au, F.L., van Galen, W.J., Middelkoop, E., Bos, J.D., and Mekkes, J.R. Fibroblasts derived from chronic diabetic ulcers differ in their response to stimulation with EGF, IGF-I, bFGF and PDGF-AB compared to controls. Eur J Cell Biol **81,** 153, 2002.
5. Tepper, O.M., Galiano, R.D., Capla, J.M., Kalka, C., Gagne, P.J., Jacobowitz, G.R., Levine, J.P., and Gurtner, G.C. Human endothelial progenitor cells from type II diabetics exhibit impaired proliferation, adhesion, and incorporation into vascular structures. Circulation **26,** 2781, 2002.
6. Terashi, H., Izumi, K., Deveci, M., Rhodes, L.M., and Marcelo, C.L. High glucose inhibits human epidermal keratinocyte proliferation for cellular studies on diabetes mellitus. Int Wound J **2,** 298, 2005.
7. Gurtner, G.C., Werner, S., Barrandon, Y., and Longaker, M.T. Wound repair and regeneration. Nature **453,** 314, 2008.
8. Stappenbeck, T.S., and Miyoshi, H. The role of stromal stem cells in tissue regeneration and wound repair. Science **324,** 1666, 2009.
9. Trottier, V., Marceau-Fortier, G., Germain, L., Vincent, C., and Fradette, J. IFATS collection: using human adipose-derived stem/stromal cells for the production of new skin substitutes. Stem Cells **26,** 2713, 2008.
10. Gimble, J.M., Katz, A.J., and Bunnell, B.A. Adipose-derived stem cells for regenerative medicine. Circ Res **100,** 1249, 2007.
11. Parker, A.M., and Katz, A.J. Adipose-derived stem cells for the regeneration of damaged tissues. Expert Opin Biol Ther **6,** 567, 2006.
12. Cao, Y., Sun, Z., Liao, L., Meng, Y., Han, Q., and Zhao, R.C. Human adipose tissue-derived stem cells differentiate into

endothelial cells *in vitro* and improve postnatal neovascularization *in vivo*. Biochem Biophys Res Commun **332,** 370, 2005.
13. Rehman, J., Traktuev, D., Li, J., Merfeld-Clauss, S., Temm-Grove, C.J., Bovenkerk, J.E., Pell, C.L., Johnstone, B.H., Considine, R.V., and March, K.L. Secretion of angiogenic and antiapoptotic factors by human adipose stromal cells. Circulation **109,** 1292, 2004.
14. Galiano, R.D., Michaels, J., Dobryansky, M., Levine, J.P., and Gurtner, G.C. Quantitative and reproducible murine model of excisional wound healing. Wound Repair Regen **12,** 485, 2004.
15. Yoshida, S., Matsumoto, K., Tomioka, D., Bessho, K., Itami, S., Yoshikawa, K., and Nakamura, T. Recombinant hepatocyte growth factor accelerates cutaneous wound healing in a diabetic mouse model. Growth Factors **22,** 111, 2004.
16. Bevan, D., Gherardi, E., Fan, T.P., Edwards, D., and Warn, R. Diverse and potent activities of HGF/SF in skin wound repair. J Pathol **203,** 831, 2004.
17. Altman, A.M., Matthias, N., Yan, Y., Song, Y.H., Bai, X., Chiu, E.S., Slakey, D.P., and Alt, E.U. Dermal matrix as a carrier for *in vivo* delivery of human adipose-derived stem cells. Biomaterials **29,** 1431, 2008.
18. Nambu, M., Kishimoto, S., Nakamura, S., Mizuno, H., Yanagibayashi, S., Yamamoto, N., Azuma, R., Nakamura, S., Kiyosawa, T., Ishihara, M., and Kanatani, Y. Accelerated wound healing in healing-impaired db/db mice by autologous adipose tissue-derived stromal cells combined with atelocollagen matrix. Ann Plast Surg **62,** 317, 2009.
19. Nie, C., Yang, D., and Morris, S.F. Local delivery of adipose-derived stem cells via acellular dermal matrix as a scaffold: A new promising strategy to accelerate wound healing. Med Hypotheses **72,** 679, 2009.
20. Kim, W.S., Park, B.S., Sung, J.H., Yang, J.M., Park, S.B., Kwak, S.J., and Park, J.S. Wound healing effect of adipose-derived stem cells: a critical role of secretory factors on human dermal fibroblasts. J Dermatol Sci **48,** 15, 2007.
21. Macri, L., Silverstein, D., and Clark, R.A. Growth factor binding to the pericellular matrix and its importance in tissue engineering. Adv Drug Deliv Rev **59,** 1366, 2007.
22. Sullivan, S.R., Underwood, R.A., Sigle, R.O., Fukano, Y., Muffley, L.A., Usui, M.L., Gibran, N.S., Antezana, M.A., Carter, W.G., and Olerud, J.E. Topical application of laminin-322 to diabetic mouse wounds. J Dermatol Sci **48,** 177, 2007.
23. Katz, A.J., Tholpady, A., Tholpady, S.S., Shang, H., and Ogle, R.C. Cell surface and transcriptional characterization of human adipose-derived adherent stromal (hADAS) cells. Stem Cells **23,** 412, 2005.
24. Parker, A.M., Shang, H., Khurgel, M., and Katz, A.J., Low serum and serum-free culture of multipotential human adipose stem cells. Cytotherapy **9,** 637, 2007.
25. Kelm, J.M., Timmins, N.E., Brown, C.J., Fussenegger, M., and Nielsen, L.K. Method for generation of homogeneous multicellular tumor spheroids applicable to a wide variety of cell types. Biotechnol Bioeng **83,** 173, 2003.
26. Banerjee, M., and Bhonde, R.R. Application of hanging drop technique for stem cell differentiation and cytotoxicity studies. Cytotechnology **51,** 1, 2006.
27. Peppa, M., Brem, H., Ehrlich, P., Zhang, J.G., Cai, W., Li, Z., Croitoru, A., Thung, S., and Vlassara, H. Adverse effects of dietary glycotoxins on wound healing in genetically diabetic mice. Diabetes **51,** 11, 2003.
28. Wu, Z., and Irizarry, R.A. Stochastic models inspired by hybridization theory for short oligonucleotide arrays. J Comput Biol **12,** 882, 2005.
29. Gentleman, R. Bioinformatics and Computational Biology Solutions Using R and Bioconductor. New York: Springer Science+Business Media, 2005.
30. Trousdale, R.K., Jacobs, S., Simhaee, D.A., Wu, J.K., and Lustbader, J.W. Wound closure and metabolic parameter variability in a db/db mouse model for diabetic ulcers. J Surg Res **151,** 100, 2009.
31. Montandon, D., D'andiran, G., and Gabbiani, G. The mechanism of wound contraction and epithelialization: clinical and experimental studies. Clin Plast Surg **4,** 325, 1977.
32. Greenhalgh, D.G. Models of wound healing. J Burn Care Rehabil **26,** 293, 2005.
33. Brown, R.L., and Greenhalgh, D.G. Mouse models to study wound closure and topical treatment of infected wounds in healing-impaired and normal healing hosts. Wound Repair Regen **5,** 198, 1997.
34. Michaels, J., Churgin, S.S., Blechman, K.M., Greives, M.R., Aarabi, S., Galiano, R.D., and Gurtner, G.C. db/db mice exhibit severe wound-healing impairments compared with other murine diabetic strains in a silicone-splinted excisional wound model. Wound Repair Regen **15,** 665, 2007.
35. Tsuboi, R., Shi, C.M., Rifkin, D.B., and Ogawa, H. A wound healing model using healing-impaired diabetic mice. J Dermatol **19,** 673, 1992.
36. Levenson, S.M., Geever, E.F., Crowley, L.V., Oates, J.F., 3rd, Berard, C.W., and Rosen, H. The healing of rat skin wounds. Ann Surg **161,** 293, 1965.
37. Falanga, V., Iwamoto, S., Chartier, M., Yufit, T., Butmarc, J., Kouttab, N., Shrayer, D., and Carson, P. Autologous bone marrow-derived cultured mesenchymal stem cells delivered in a fibrin spray accelerate healing in murine and human cutaneous wounds. Tissue Eng **13,** 1299, 2007.
38. Kirchner, L.M., Meerbaum, S.O., Gruber, B.S., Knoll, A.K., Bulgrin, J., Taylor, R.A., and Schmidt, S.P. Effects of vascular endothelial growth factor on wound closure rates in the genetically diabetic mouse model. Wound Repair Regen **11,** 127, 2003.
39. Tsuboi, R., Shi, C.M., Sato, C., Cox, G.N., and Ogawa, H. Co-administration of insulin-like growth factor (IGF)-I and IGF-binding protein-1 stimulates wound healing in animal models. J Invest Dermatol **104,** 199, 1995.
40. Lee, P.Y., Chesnoy, S., and Huang, L. Electroporatic delivery of TGF-beta1 gene works synergistically with electric therapy to enhance diabetic wound healing in db/db mice. J Invest Dermatol **123,** 791, 2004.
41. Telgenhoff, D., and Shroot, B. Cellular senescence mechanisms in chronic wound healing. Cell Death Differ **12,** 695, 2005.
42. Brem, H., Kodra, A., Golinko, M.S., Entero, H., Stojadinovic, O., Wang, V.M., Sheahan, C.M., Weinberg, A.D., Woo, S.L.C., Ehrlich, H.P., and Tomic-Canic, M. Mechanism of sustained release of vascular endothelial growth factor in accelerating experimental diabetic healing. J Invest Dermatol **129,** 2275, 2009.
43. Rahman, S., Patel, Y., Murray, J., Patel, K.V., Sumathipala, R., Sobel, M., and Wijelath, E.S. Novel hepatocyte growth factor (HGF) binding domains on fibronectin and vitronectin coordinate a distinct and amplified Met-integrin induced signalling pathway in endothelial cells. BMC Cell Biol **6,** 8, 2005.
44. Clark, R.A.F. Synergistic signalling from extracellular matrix-growth factor complexes. J Invest Dermatol **128,** 1354, 2008.
45. Kilroy, G.E., Foster, S.J., Wu, X., Ruiz, J., Sherwood, S., Heifetz, A., Ludlow, J.W., Stricker, D.M., Potiny, S., Green, P., Halvorsen, Y.D., Cheatham, B., Storms, R.W., and

Gimble, J.M. Cytokine profile of human adipose-derived stem cells: expression of angiogenic, hematopoietic, and pro-inflammatory factors. J Cell Physiol **212,** 702, 2007.
46. Planat-Benard, V., Silvestre, J.S., Cousin, B., André, M., Nibbelink, M., Tamarat, R., Clergue, M., Manneville, C., Saillan-Barreau, C., Duriez, M., Tedgui, A., Levy, B., Pénicaud, L., and Casteilla, L. Plasticity of human adipose lineage cells toward endothelial cells. Circulation **109,** 23, 2004.
47. Miranville, A., Heeschen, C., Sengenes, C., Curat, C.A., Busse, R., and Bouloumié, A. Improvement of postnatal neovascularization by human adipose tissue-derived stem cells. Circulation **110,** 349, 2004.
48. Sengenès, C., Miranville, A., Maumus, M., de Barros, S., Busse, R., and Bouloumié, A. Chemotaxis and differentiation of human adipose tissue CD34+/CD31- progenitor cells: role of stromal derived factor-1 released by adipose tissue capillary endothelial cells. Stem Cells **25,** 2269, 2007.
49. Mitchell, J.B., McIntosh, K., Zvonic, S., Garrett, S., Floyd, Z.E., Kloster, A., Di Halvorsen, Y., Storms, R.W., Goh, B., Kilroy, G., Wu, X., and Gimble, J.M., Immunophenotype of human adipose-derived cells: temporal changes in stromal-associated and stem cell–associated markers. Stem Cells **24,** 376, 2006.
50. Fuchs, E., Tumbar, T., and Guasch, G. Socializing with the neighbors: stem cells and their niche. Cell **116,** 769, 2004.
51. Kim, W.-S., Park, B.-S., and Sung, J.-H. The wound-healing and antioxidant effects of adipose-derived stem cells. Expert Opin Biol Ther **9,** 879, 2009.
52. Kelm, J.M., Sanchez-Bustamante, C.D., Ehler, E., Hoerstrup, S.P., Djonov, V., Ittner, L., and Fussenegger, M. VEGF profiling and angiogenesis in human microtissues. J Biotech **118,** 213, 2005.
53. Griffiths, M., Ojeh, N., Livingstone, R., Price, R., and Navsaria, H. Survival of Apligraf in acute human wounds. Tissue Eng **10,** 1180, 2004.
54. Amos, P.J., Shang, H., Bailey, A.M., Taylor, A., Katz, A.J., and Peirce, S.M. IFATS collection: the role of human adipose-derived stromal cells in inflammatory microvascular remodeling and evidence of a perivascular phenotype. Stem Cells **26,** 2682, 2008.
55. Barber, C., Watt, A., Pham, C., Humphreys, K., Penington, A., Mutimer, K., Edwards, M., and Maddern, G. Influence of bioengineered skin substitutes on diabetic foot ulcer and venous leg ulcer outcomes. J Wound Care **17,** 12, 2008.
56. Ehrenreich, M., and Ruszczak, Z. Update on tissue-engineered biological dressings. Tissue Eng **12,** 9, 2006.

Address correspondence to:
Adam J. Katz, M.D.
Department of Plastic and Reconstructive Surgery
University of Virginia
P.O. Box 800376
Charlottesville, VA 22908

Email: ajk2f@virginia.edu

Received: September 14, 2009
Accepted: December 23, 2009
Online Publication Date: February 3, 2010